

GRB Theory in the Fermi Era

J. Granot

on behalf of the Fermi LAT and GBM collaborations

Centre for Astrophysics Research, University of Hertfordshire, College Lane, Hatfield AL10 9AB, UK

Before the launch of the Fermi Gamma-ray Space Telescope there were only a handful of gamma-ray bursts (GRBs) detected at high energies (above 100 MeV), while several different suggestions have been made for possible high-energy emission sites and mechanisms. Here I briefly review some of the theoretical expectations for high-energy emission from GRBs, outline some of the hopes for improving our understanding of GRB physics through Fermi observations of the prompt GRB emission or the early afterglow (first few hours after the GRB), and summarize what we have learned so far from the existing Fermi GRB observations (over its first half-year of operation). Highlights include the first detection of $> \text{GeV}$ emission from a short GRB, as well as detailed temporal and spectral information for the first GRB with $> \text{GeV}$ emission and a measured redshift, that has the highest measured apparent (isotropic equivalent) radiated energy output (for any GRB), the largest lower limit on the bulk Lorentz factor of the emitting region, and constrains possible Lorentz invariance violation by placing a robust lower limit on the quantum gravity mass.

1 Introduction: pre-Fermi high-energy GRB observations

High-energy emission from GRBs was first detected by the Energetic Gamma-Ray Experiment Telescope (EGRET) on-board the Compton Gamma-Ray Observatory (CGRO; 1991–2000). While EGRET detected only five GRBs with its Spark Chambers (20 MeV – 30 GeV) and a few GRBs with its Total Absorption Shower Counter (TASC; 1 – 200 MeV), these events already showed diversity. Most noteworthy are GRB 940217, with high-energy emission lasting up to ~ 1.5 hr after the GRB including an 18 GeV photon after ~ 1.3 hr,¹ and GRB 941017 which had a distinct high-energy spectral component² detected up to ~ 200 MeV with $\nu F_\nu \propto \nu$. This high-energy spectral component had ~ 3 times more energy and lasted longer (~ 200 s) than the low-energy (hard X-ray to soft gamma-ray) spectral component (which lasted several tens of seconds), and may be naturally explained as inverse-Compton emission from the forward-reverse shock system that is formed as the ultra-relativistic GRB outflow is decelerated by the external medium.^{3,4} Nevertheless, better data are needed in order to determine the origin of such high-energy spectral components more conclusively. The Italian experiment Astro-rivelatore Gamma a Immagini LEggero (AGILE; 2007–) has detected GRB 080514B at energies up to ~ 300 MeV, and the high-energy emission lasted longer (> 13 s) than the low-energy emission (~ 7 s).⁵

Fermi has raised great expectations for probing the high-energy emission from GRBs as its Large Area Telescope (LAT; from 20 MeV to > 300 GeV) significantly improves upon previous missions, mainly in terms of its large effective area, small dead-time and large field of view. Together with its Gamma-ray Burst Monitor (GBM; 8 keV – 40 MeV) Fermi has an unprecedented energy range of ~ 7.5 decades, which is extremely useful for studying the GRB emission.

2 Expectations from Fermi

Prompt emission: most people hoped for, or even expected, the detection of a distinct high-energy spectral component. Such a detection can shed light on the prompt GRB emission mechanism at low energies (for which the νF_ν spectrum which typically peaks at E_{peak} of around a few hundred keV), which is still unclear, as well as the emission mechanism at high energies. A high-energy spectral component may arise either from leptonic processes, namely inverse-Compton scattering by the same population of relativistic electrons responsible for the observed low-energy prompt emission,^{6,7} or from hadronic processes⁸ such as proton synchrotron, photo-pair production, and pion production via photo-meson interaction or p-p collisions, that may lead to pair cascades. Moreover, if the energy output in such a high-energy spectral component is comparable to or even larger than that in the low-energy spectral component (as seen by EGRET for GRB 941017) then this will increase the already very tight requirements on the source in terms of the total radiated energy and the efficiency of the gamma-ray emission.⁹

Many hopes were raised to detect a high-energy spectral cutoff or steepening due to opacity to pair production ($\gamma\gamma \rightarrow e^+e^-$) at the source.^{10,11} Such a detection would determine $\Gamma^{-2\beta} R$, where Γ and R are the bulk Lorentz factor and distance from the source of the emitting region, and β is the (directly measurable) high-energy photon index. Thus, it would determine both Γ and R for models (such as the popular internal shocks model) in which $R \sim \Gamma^2 c \Delta t$, where Δt is the observed variability time of the prompt GRB emission, or test whether this relation holds if Γ can be estimated independently (e.g. from the afterglow onset time).

Longer lived high-energy emission: several possible mechanisms have been suggested for long lived high-energy emission from GRBs, which may be detectable well after the end of the prompt GRB emission. Synchrotron self-Compton (SSC – the inverse-Compton scattering of seed synchrotron photons emitted by the same population of relativistic electrons) emission at GeV energies is expected from the afterglow (i.e. the long lived forward shock going into the external medium). Early on, when there is also a reverse shock going into the ejecta, it can also produce inverse-Compton emission at high energies, either via SSC, or by “external-Compton” (EC; inverse-Compton scattering in which the seed photons are produced in a different region), where reverse shock electrons scatter the forward shock synchrotron photons, or vice versa.¹² In some models^{13,14} the reverse shock can be long-lived, lasting for hours or even days, in which case such high-energy emission involving the reverse shock would be similarly long-lived. Other inverse-Compton processes involving two different emission regions have also been suggested. In particular, the *Swift* satellite detects flares in the early X-ray afterglow in about half of the GRBs it observes, typically from hundreds to thousands of seconds after the GRB. These X-ray flares are often attributed to sporadic late-time activity of the central source, and are believed to be emitted at a smaller radius than that of the contemporaneous afterglow shock. In this scenario, EC may operate where afterglow electrons scatter flare photons¹⁵ or vice versa.¹⁶

Another mechanism that may produce long lived high-energy emission is a pair echo. In this scenario \gtrsim TeV photons that escape the source pair produce with the cosmic infrared background (or the cosmic microwave background – CMB), producing e^+e^- pairs with \sim TeV energies, that in turn inverse-Compton scatter CMB photons to \sim GeV energies. This emission can potentially be detected up to thousands of seconds after the GRB, if the inter-galactic magnetic fields are sufficiently low ($\lesssim 10^{-20}$ G for a correlation length of ~ 1 Mpc).^{17,7} Finally, hadronic processes involving high-energy cosmic-rays accelerated in the prompt GRB emission region, or in the afterglow shock, could potentially produce long-lived high-energy emission.

High-energy GRB observations by Fermi on a time scale of up to hours after the GRB can either detect some of these emission components or alternatively place interesting limits on them. In both cases, the hope is that Fermi would thus be able to constrain the physical conditions at the source and help determine the dominant high-energy emission mechanisms.

3 First results from Fermi

GBM: the GBM has a very wide field of view (full sky, half of which is occulted by the Earth at any time) and is only slightly less sensitive than the Burst and Transient Source Experiment (BATSE, that was on-board the CGRO), thus resulting in a comparable (only slightly lower) GRB detection rate of $\sim 250 \text{ yr}^{-1}$, where $\sim 18\%$ of them are of the short duration spectrally hard class of GRBs. A good fraction of GBM GRBs are within the LAT field of view.

LAT GRB detection rate: during the first ~ 9 months of operation Fermi LAT has clearly detected high-energy emission from 7 GRBs, corresponding to a detection rate of $\sim 9 \text{ yr}^{-1}$. A detailed comparison to the expected detection rate requires specifying the number of detected photons above a certain energy. The preliminary results (which suffer from a large statistical uncertainty due to the small number of detected GRBs) are $\sim 7-8 \text{ yr}^{-1}$ ($\sim 1-2 \text{ yr}^{-1}$) with at least 10 photons above 100 MeV (1 GeV). This is compatible (perhaps slightly lower but well within the errors) with the expected rate¹⁸ based on a sample of bright BATSE GRBs for which the fit to a Band spectrum over the BATSE energy range (30 keV – 2 MeV) is extrapolated into the LAT energy range, and excluding cases with a rising νF_ν spectrum at high energies (i.e. a high-energy photon index $\beta > -2$).^a This suggests that, on average, there is no significant excess (perhaps even a slight deficit) of high-energy emission in the LAT energy range relative to such an extrapolation from lower energies. Note that this expected detection rate (that is close to the observed rate) is smaller than that for a larger sample of BATSE bursts that includes events that are dimmer in the BATSE range, some of which have $\beta \gtrsim -2$ and would be detectable by the LAT upon extrapolation, thus increasing the expected LAT detection rate. It should be noted, however, that for such GRBs that are relatively dim in the BATSE range it is hard to determine the value of β very accurately, and it might suffer from some systematic error.

GRB 081024B: this GRB was detected by the LAT with more than 10 photons above 100 MeV, and is the first clearly short GRB that is detected at high energies (up to a few GeV). Its spectrum is consistent with a single Band function, similar to the LAT long GRBs. Its high-energy emission ($> 100 \text{ MeV}$) lasts about 3 s, while its low-energy emission goes back to background levels after 0.8 s. Even though it was not possible to determine its redshift (due to the lack of an afterglow detection), the lack of a high-energy cutoff in its spectrum up to the highest detected photon energies implies a fairly high lower limit on its bulk Lorentz factor for any reasonable redshift: $\Gamma_{\min}(z = 0.1) \approx 150$ while $\Gamma_{\min}(z = 3) \approx 900$. These values are significantly higher than the pre-Fermi conservative estimates for short GRBs¹⁹, that were based on the prompt emission spectrum of many short BATSE GRBs being well-fit by a power-law with a high-energy exponential cutoff, where such an exponential cutoff at high energies results in a much lower Γ_{\min} compared to a (reasonably hard) power-law at high energies.

4 A minimal Lorentz factor of the emitting region from compactness arguments

The large isotropic equivalent luminosities ($L \sim 10^{50} - 10^{53} \text{ erg s}^{-1}$) and short observed variability time ($\Delta t \sim 1 \text{ ms} - 1 \text{ s}$) of GRBs would imply a huge opacity to pair production ($\gamma\gamma \rightarrow e^+e^-$) within the source ($\tau_{\gamma\gamma} \gg 1$) if the source (i.e. the emitting region) is at rest or moving at a sub-relativistic velocity relative to us. Neglecting cosmological factors of $(1+z)$ for simplicity, an order of magnitude estimate of the optical depth at a dimensionless photon energy $\varepsilon \equiv E_{\text{ph}}/m_e c^2$ gives $\tau_{\gamma\gamma} \sim \sigma_T n_{\text{ph}}(1/\varepsilon) R \sim \sigma_T L_{1/\varepsilon} / (4\pi m_e c^3 R) \gtrsim 10^{14} (L_{1/\varepsilon} / 10^{51} \text{ erg s}^{-1}) (\Delta t / 1 \text{ ms})^{-1}$, where $R \lesssim c\Delta t$ is the source size and $n_{\text{ph}}(1/\varepsilon)$ is the number density of the target photons (near the threshold for pair production) that provide most of the opacity. Such a huge optical depth would

^aSuch a hard high-energy photon index may be an artifact of the limited energy range of the fit to BATSE data, and even if such a hard spectrum is present in the BATSE range it is not very likely that νF_ν continues to smoothly rise well into the LAT energy range.

result in a (quasi-) thermal spectrum, in stark contrast with the significant high-energy power-law tail observed in most GRBs. This is known as the compactness problem.²⁰ Its solution is that the source moves toward us at a very high Lorentz factor, $\Gamma \gg 1$. This reduces $\tau_{\gamma\gamma}$ due to three effects. First, the threshold for pair production is $\varepsilon_1\varepsilon_2 > 2/(1 - \cos\theta_{12})$ where ε_1 and ε_2 are the two photon energies and θ_{12} is the angle between their directions. For a source at rest, $\theta_{12} \sim 1$ and $\varepsilon_1\varepsilon_2 \gtrsim 1$, while for a relativistic source $\theta_{12} \sim 1/\Gamma$ (due to relativistic beaming) and $\varepsilon_1\varepsilon_2 \gtrsim \Gamma^2$ (in the source rest frame $\theta'_{12} \sim 1$ and $\varepsilon'_1\varepsilon'_2 \gtrsim 1$ where $\varepsilon' \sim \varepsilon/\Gamma$). Thus $L_{1/\varepsilon}$ is replaced by $L_{\Gamma^2/\varepsilon} = L_{1/\varepsilon}\Gamma^{2(1+\beta)}$, adding a factor of $\sim \Gamma^{2(1+\beta)}$ to the expression for $\tau_{\gamma\gamma}$, where β is the high-energy photon index ($L_\varepsilon = L_0\varepsilon^{1+\beta}$ in the relevant energy range). Second, R should now represent the distance in the lab frame over which n_{ph} is large enough to significantly contribute to $\tau_{\gamma\gamma}$, i.e. roughly the distance of the emitting region from the source, and $R \lesssim \Gamma^2 c\Delta t$ is possible since $\Delta t \sim R/(c\Gamma^2)$ is the time delay in the arrival of photons from an angle of $\sim 1/\Gamma$ from the line of sight relative to the line of sight itself for an emitting region with a radius of curvature $\sim R$ (in the lab frame), as well as the difference in arrival time of two photons emitted along the line of sight over a radial interval $\Delta R \sim R$. This adds a factor of $\sim \Gamma^{-2}$ to the expression for $\tau_{\gamma\gamma}$. Finally, there is a factor of $1 - \cos\theta_{12} \sim \Gamma^{-2}$ in the differential expression for $\tau_{\gamma\gamma}$, due to the rate at which the photons pass each other and have a chance of interacting (exactly parallel photons will never interact). This results in an additional factor of $\sim \Gamma^{-2}$ in the expression for $\tau_{\gamma\gamma}$. Altogether, $\tau_{\gamma\gamma}$ includes a factor of $\sim \Gamma^{2(1-\beta)}$, and since typically $-\beta \sim 2 - 3$, this typically requires $\Gamma > \Gamma_{\text{min}} \sim 100$ in order to achieve $\tau_{\gamma\gamma} < 1$. In particular, when there is no high-energy cutoff or steepening in the spectrum up to an observed photon energy of ε_{max} , then the requirement that $\tau_{\gamma\gamma}(\varepsilon_{\text{max}}) < 1$ leads to $\Gamma_{\text{min}} \propto (L_0/\Delta t)^{1/2(1-\beta)}(\varepsilon_{\text{max}})^{(-1-\beta)/2(1-\beta)}$.

5 GRB 080916C

GRB 080916C was the second GRB detected by the LAT and the brightest so far. It had > 3000 raw LAT counts (after background subtraction) in the first 100 s, with 145 events above 100 MeV that could be used for spectral analysis, and 14 photons above 1 GeV.²¹ The accurate localization by the LAT (to within $\sim 0.1^\circ$) enabled the detection of its X-ray afterglow after 17 hr in a follow-up observation by the *Swift* X-ray telescope,²² which in turn provided a much better localization (to within $1.9''$) that enabled follow-up observations by ground based telescopes and the detection of the optical/NIR afterglow by the Gamma-Ray Burst Optical/Near-Infrared Detector (GROND), which was able to measure a photometric redshift of $z = 4.35 \pm 0.15$.²³

Energetics and beaming: GRB 080916C was a very bright long GRB. It had a very high fluence of $f = 2.4 \times 10^{-4}$ erg cm $^{-2}$, corresponding to an isotropic equivalent energy output of $E_{\gamma,\text{iso}} \approx 8.8 \times 10^{54}$ erg $\approx 4.9M_\odot c^2$, which is the highest measured so far for any GRB, and strongly suggests that the outflow was collimated into a narrow jet, in order to alleviate the otherwise very extreme energy requirements from the source.

Spectral evolution: the time resolved spectrum of the prompt emission in GRB 080916C was analyzed in five different time bins (chronologically labeled **a-e**; see *left* and *middle panels* of Fig. 1) and found to be well-fit by a single Band spectrum (featuring a smooth transition between two power-law segments) in a combined fit of the LAT and GBM data. The peak of the νF_ν spectrum, E_{peak} , first increases between the first and second time bins, and then gradually decreases with time (see *middle panel* of Fig. 1). The photon indices at low energies, α , and at high energies, β , both change between the first and second time bins, α becoming softer and β becoming harder, and are then consistent with remaining constant in time.

Implications of a single dominant spectral component: the fact that the spectrum in time bins **a-e** is consistent with a single Band function suggests that a single spectral component, arising from a single emission mechanism, dominates throughout the observed energy range,

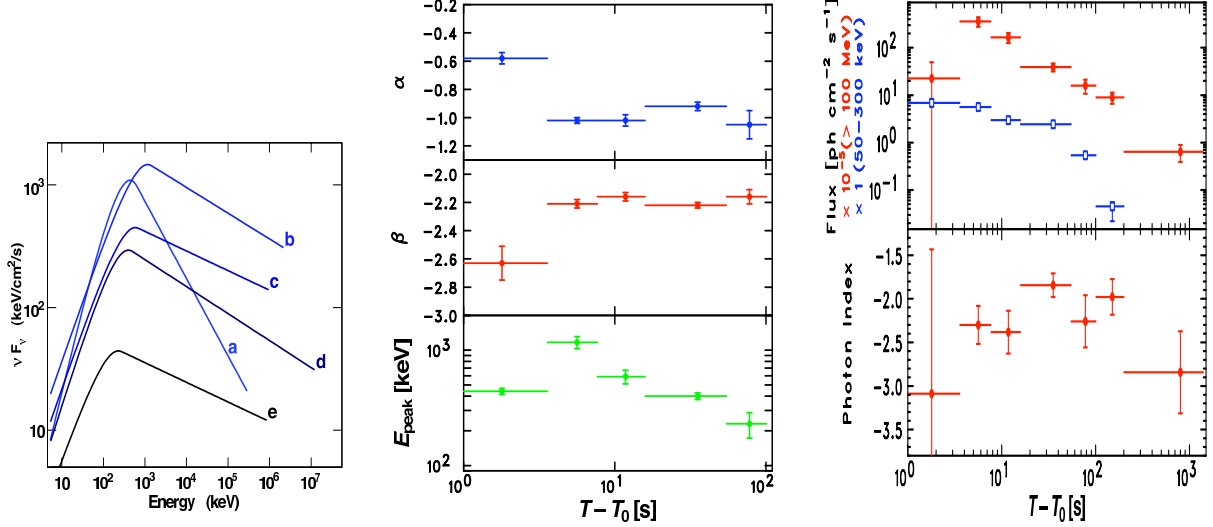


Figure 1: Spectral evolution of GRB 080916C.²¹ **Left panel:** The best-fit model νF_ν spectra for all five time intervals. The changing shapes show the evolution of the spectrum over time. The curves end at the energy of the highest-energy photon observed in each time interval. **Middle panel:** Fit parameters for the Band function – the photon index at low (α) and high (β) energies, and the photon energy (E_{peak}) where the νF_ν spectrum peaks – as a function of time. Error bars indicate 1σ uncertainty. **Right panel:** Fluxes (*top*) for the energy ranges 50 – 300 keV (blue open squares) and > 100 MeV (red solid squares) and power-law index as a function of the time from the GRB trigger time T_0 to $T_0 + 1400$ s [(*bottom*) LAT data only].

which cover 6 decades in energy (roughly 10 keV – 10 GeV). This provides interesting constraints on any emission mechanism. For example, if the observed emission is synchrotron radiation, then an SSC component may peak in the LAT energy range, and the fact that it is not detected suggests that either (i) it has a lower luminosity, its peak νF_ν being at least ~ 10 times lower than that of the synchrotron component, if the SSC component peak around several GeV, implying at least ~ 10 times more energy in relativistic electrons than in the magnetic field in the emission region, or (ii) the SSC component may have a comparable or even higher luminosity than that of the synchrotron component if it peaks well above 10 GeV, in which case it will be hard to detect it due to the smaller number of photons at higher energies and attenuation due to pair production with the extra-Galactic background light (EBL).

EBL: in time bin **d** there is weak evidence for a possible high-energy excess relative to a Band spectrum.²¹ The chance probability of such an excess is 1%, and taking into account the 5 trials (for bins **a-e**) it increases to 5% (or 2σ). For some EBL models the optical depth for pair production with the EBL of the highest energy detected photon, $13.22^{+0.70}_{-1.54}$ GeV, is $\tau_{\gamma\gamma} \sim 3-4$, in which case the significance of an additional high-energy spectral component would be increased to $\sim 3-4 \sigma$. Such a spectral component may increase the already extreme apparent radiated energy in GRB 080916C. However, for many other EBL models $\tau_{\gamma\gamma}(13 \text{ GeV}) \ll 1$, resulting in a mere 2σ hint of a possible excess, which is not very significant.

Delayed high-energy onset: the high-energy emission in GRB 080916C starts $\sim 4-5$ s after the low-energy emission. After the onset of the LAT emission it quickly rises to a bright sharp peak – the main peak in the LAT lightcurve, which coincides with the second peak in the GBM lightcurve (in time bin **b**). If indeed the observed spectrum in the GBM and LAT energy range is dominated by a single spectral component, as suggested by the fact that it is well-fit by a single Band spectrum, then the delayed HE onset may be attributed mainly to a change in the high-energy photon index β between the first and second pulses in the GBM lightcurve (as was measured; see Fig. 1). This, in turn, may naturally occur if these two pulses originated in two distinct physical regions (e.g. two sets of colliding shells in the internal shocks model) with

different physical conditions, resulting in a different power-law index of the energy distribution of the accelerated relativistic electron population that is responsible for the observed emission.

Opacity effects do not work well as an alternative explanation since there is no sign of a high-energy cutoff or steepening in the spectrum (that must be present in the observed energy range in order for opacity effects to be the major cause for the observed delayed onset).

Contribution from an additional spectral component at high energies may be possible if together with the spectral component that dominates at low energies the combined spectrum is still well-fit by a single Band function (which is not always that easy to achieve). In this case, however, it is not obvious why the effective value of β (or the luminosity ratio of the two components) should remain constant for the remainder of the GRB (time bins **b-e**). If the main LAT peak is attributed to emission from the same physical region as the first GBM peak (e.g. due to the gradual acceleration of high-energy protons or heavier ions that produce pair cascades) then it is not clear why it should coincide with the second GBM peak or why the main LAT peak is as sharp as it is (as a much smoother peak would be expected in this case). Altogether, the exact cause for the delayed high-energy onset is still not clear, and more detailed modeling could help address this question.

Long lived high-energy emission: while the low-energy emission lasted several tens of seconds, with some low level emission detected up to 200 s after the GRB trigger time, high-energy emission was detected by the LAT for more than 1000 s. In particular, the LAT detected emission above 100 MeV in two additional time bins (just after time bins **a-e**), 100 – 200 s and 200 – 1400 s (see *right panel* of Fig. 1). The > 100 MeV LAT flux decayed as $t^{-1.2\pm 0.2}$ from several seconds and up to 1400 s, while during the last time bin (200 – 1400 s) the photon index was $\beta = -2.8 \pm 0.5$. The GBM flux decayed more slowly ($\sim t^{-0.6}$) up to ~ 55 s, and faster ($\sim t^{-3.3}$) at later times (until fading below detection threshold around 200 s).

Different possible mechanisms may account for such a long lived high-energy emission. A natural possibility is afterglow SSC emission, but spectral hardening is expected when this component becomes dominant, and this is not seen in the data. Some time delay may be caused by scattering of photons emitted at a smaller radius¹⁵ (e.g. an inner set of colliding shells in the internal shock model) or due pair cascades induced by ultra-relativistic ions accelerated in the prompt emission region.²⁴ In both cases, however, it might be hard to produce the relatively slow decay rate, due to adiabatic losses on a much shorter timescale (that of the observed prompt emission pulses). Other options are scattering of photons from early X-ray flares (undetected in this case, but detected by *Swift* in many other GRBs) by afterglow electrons, or a pair echo. It is hard to conclusively determine the exact mechanism at work here, but further study may help distinguish between the different possibilities.

Comparison to other GRBs: while there is a hint of a delayed onset of the high-energy emission in other LAT GRBs, in those cases it is not nearly as significant as in GRB 080916C. However, a longer duration of the high-energy emission compared to the low-energy emission appears in most LAT GRBs so far, and seems to be a common feature in GRBs. Moreover, it also appeared in EGRET GRBs (especially in GRB 940217) and in the AGILE GRB 080514B. It is hard to tell whether the longer lived high-energy emission is from a similar mechanism in all these cases or from different mechanisms in different GRBs, due to the rather low photon statistics of this long-lived emission and the lack of good broad-band monitoring of the contemporaneous afterglow emission at lower frequencies (mainly X-ray and optical). Nevertheless, such broad-band coverage may improve in the near future and help in distinguishing between the different possible physical origins of the long lasting high-energy emission.

Minimum Lorentz factor: the very high isotropic equivalent luminosity together with the fact that the spectrum did not show any significant deviation from a Band spectrum up to the highest observed photon energies (of $E_{\max} \gtrsim$ a few GeV) require a very large bulk Lorentz factor of the emitting region, $\Gamma > \Gamma_{\min}$, in order for the optical depth to pair production in the source

to satisfy $\tau_{\gamma\gamma}(E_{\max}) < 1$ (see § 4). For time bin **d** this implies $\Gamma_{\min} = 608 \pm 15$. For time bin **b** $\Gamma_{\min} = 887 \pm 21$ for an observed variability time of $\Delta t = 2$ s (the time for a factor of ~ 2 GBM flux variation). A more careful inspection of the low-energy lightcurve in time bin **b** shows significant variability at least down to timescales of 0.5 s, and adopting $\Delta t = 0.5$ s results in $\Gamma_{\min} \approx 1100$. Even the more conservative value of $\Gamma_{\min} \approx 900$ is more than twice the previous largest Γ_{\min} for any other GRB from opacity considerations.¹⁰ Moreover, our limit is more robust than previous ones, since in our case the target photons that provide the opacity for the highest energy observed photon are within the observed energy range ($E_{\text{ph}} \ll E_{\max}$), while for previous limits they were well above the observed energy range ($E_{\text{ph}} \gg E_{\max}$), and therefore it was not clear whether they were indeed present at the source. Note that for the conservative assumption that the photon spectrum reaches only up to E_{\max} , $\Gamma_{\min} \lesssim (1+z)E_{\max}/m_e c^2 \approx 200(1+z)(E_{\max}/100 \text{ MeV})$, and therefore a large Γ_{\min} requires the detection of high-energy photons. Our lower limit on Γ for time bin **b** implies a fairly large emission radius, $R \sim \Gamma^2 c \Delta t / (1+z) \gtrsim 10^{16}$ cm.

Limits on Lorentz invariance violation: some quantum gravity models predict energy dispersion in the propagation speed of photons, where high-energy photons travel slower^b than low-energy photons.²⁵ The Lorentz invariance violating terms in the dependence of the photon momentum p_{ph} on the photon energy E_{ph} can be expressed as a power series,

$$\frac{p_{\text{ph}}^2 c^2}{E_{\text{ph}}^2} - 1 = \sum_{k=1}^{\infty} \left(\frac{E_{\text{ph}}}{\xi_k M_{\text{Planck}} c^2} \right)^k = \sum_{k=1}^{\infty} \left(\frac{E_{\text{ph}}}{M_{\text{QG},k} c^2} \right)^k, \quad (1)$$

in the ratio of E_{ph} and a typical energy scale $M_{\text{QG},k} c^2 = \xi_k M_{\text{Planck}} c^2$ for the k^{th} order, which is expected to be of the order of the Planck scale, $M_{\text{Planck}} = (\hbar c/G)^{1/2} \approx 1.22 \times 10^{19}$ GeV/ c^2 . That is, $\xi_k \sim 1$ may naively be expected for the coefficients that are not infinite (some terms may not appear in this sum). Since we observe photons of energy well below the Planck scale, the dominant Lorentz invariance violating term is associated with the lowest order non-zero term in the sum, of order n , which is usually assumed to be either first order ($n = 1$) or second order ($n = 2$). The photon propagation speed is given by the corresponding group velocity,

$$v_{\text{ph}} = \frac{\partial E_{\text{ph}}}{\partial p_{\text{ph}}} \approx c \left[1 - \frac{n+1}{2} \left(\frac{E_{\text{ph}}}{M_{\text{QG},n} c^2} \right)^n \right]. \quad (2)$$

Taking into account cosmological effects, this induces a time delay in the arrival of a high-energy photon of energy E_{h} , compared to a low-energy photon of energy E_{l} , of²⁶

$$\Delta t \approx \frac{(1+n)}{2H_0} \frac{(E_{\text{h}}^n - E_{\text{l}}^n)}{(M_{\text{QG},n} c^2)^n} \int_0^z \frac{(1+z')^n}{\sqrt{\Omega_M(1+z')^3 + \Omega_\Lambda}} dz'. \quad (3)$$

We apply this formula to the highest energy photon detected in GRB 080916C, with an energy of $E_{\text{h}} = 13.22_{-1.54}^{+0.70}$ GeV, which arrived at $t = 16.54$ s after the GRB trigger (i.e. after the onset of the hard X-ray to soft gamma-ray, sub-MeV emission: $E_{\text{l}} \sim 0.1$ MeV). Since we have $E_{\text{h}}/E_{\text{l}} \sim 10^5 \gg 1$, the term E_{l}^n in eq. (3) can be neglected, and $\Delta t \propto (E_{\text{h}}/M_{\text{QG},n})^n$. Since it is hard to associate the highest energy photon with a particular spike in the low-energy lightcurve, we make the conservative assumption that it was emitted sometime between the GRB trigger and the time that it was observed, i.e. $\Delta t \leq t$. This results in the following limits²¹ for $n = 1$,

$$M_{\text{QG},1} > (1.55 \pm 0.04) \times 10^{18} \left(\frac{E_{\text{h}}}{13.22 \text{ GeV}} \right) \left(\frac{\Delta t}{16.54 \text{ s}} \right)^{-1} \text{ GeV}/c^2, \quad (4)$$

^bIn principle they could also travel faster (or even faster in some photon energies and slower in others). For GRB 080916C, however, there is no high-energy photon detected before the onset of the low-energy emission (i.e. the GRB trigger), and in fact the first of the 14 photons with energies above 1 GeV arrives several seconds after the GRB trigger. Therefore, a comparable or perhaps an even somewhat stricter limit may be put on such a “negative delay” in the arrival time of high-energy photons relative to low-energy photons.

and for $n = 2$, $M_{\text{QG},2} > (9.66 \pm 0.22) \times 10^8 (E_h/13.22 \text{ GeV})(\Delta t/16.54 \text{ s})^{-1/2} \text{ GeV}/c^2$. Our limit for $n = 1$ is the strictest of its kind, and only a factor of 10 below the Planck mass.

6 Conclusions

Fermi has raised great expectations that, similar to previous major new relevant space missions, it would also significantly contribute to the progress in the GRB field. The main expectations are to improve our understanding of the prompt GRB emission mechanism and the physical properties of the emission region, possibly by observing a distinct high-energy spectral component or signatures of opacity to pair production in the source, as well as improving our understanding of the early afterglow. While most of these hopes will have to wait a bit longer, Fermi has already provided some very interesting initial results during its first half-year of operation. The spectrum of most GRBs detected so far by both the GBM and the LAT is consistent with a single Band function, suggestive of a single dominant emission mechanism in the observed energy range, as is also suggested by the LAT GRB detection rate. Longer lived high-energy emission compared to the low-energy emission (in some cases lasting $> 10^3$ s) appears to be common in LAT GRBs. Particularly interesting LAT GRBs are GRB 081024B, the first clearly short GRB detected above 1 GeV, and the exceptionally bright and energetic GRB 080916C that provided a wealth of information leading to tight lower limits on the bulk Lorentz factor of the emitting region and the quantum gravity mass. Finally, there is still a lot to look forward to from Fermi.

Acknowledgments

The author gratefully acknowledges a Royal Society Wolfson Research Merit Award.

References

1. K. Hurley *et al.*, *Nature* **372**, 652 (1994).
2. M. M. González *et al.*, *Nature* **424**, 749 (2003).
3. J. Granot and D. Guetta, *Astrophys. J.* **598**, L11 (2003).
4. A. A. Pe'er, E. Waxman, *Astrophys. J.* **613**, 448 (2004).
5. A. Giuliani *et al.*, *Aston. & Astrophys.* **491**, L25 (2008).
6. H. Papathanassiou and P. Mészáros, *Astrophys. J.* **471**, L91 (1996).
7. D. Guetta and J. Granot, *Astrophys. J.* **585**, 885 (2003).
8. M. Bottcher and C. Dermer, *Astrophys. J.* **499**, L131 (1998).
9. J. Granot, A. Königl and T. Piran, *Mon. Not. R. Astron. Soc.* **370**, 1946 (2006).
10. Y. Lithwick and R. Sari, *Astrophys. J.* **555**, 540 (2001).
11. J. Granot, J. Cohen-Tanugi and E. do Couto e Silva, *Astrophys. J.* **677**, 92 (2008).
12. X.Y. Wang, Z.G. Dai and T. Lu, *Astrophys. J.* **556**, 1010 (2001).
13. R. Sari and P. Mészáros, *Astrophys. J.* **535**, L33 (2000).
14. F. Genet, F. Daigne and R. Mochkovitch, *Mon. Not. R. Astron. Soc.* **381**, 732 (2007).
15. X.Y. Wang, Z. Li and P. Mészáros, *Astrophys. J.* **641**, L89 (2006).
16. A. Panaitescu, *Mon. Not. R. Astron. Soc.* **383**, 1143 (2008).
17. R. Plaga, *Nature* **374**, 430 (1995).
18. D. L. Band *et al.*, *Astrophys. J.* accepted (2009)
19. E. Nakar, *Phys. Rep.* **442**, 166 (2007).
20. M. Ruderman, *Ann. NY Acad. Sci.* **262**, 164 (1975).
21. A. B. Abdo *et al.*, *Science* **323**, 1688 (2009).
22. M. Perri *et al.*, GCN Circ. 8261 (2008)
23. J. Greiner *et al.*, *preprint*, <http://arxiv.org/abs/0902.0761> (2009).

24. C. D. Dermer and A. Atoyan, *New J. Phys.* **8**, 122 (2006).
25. G. Amelino-Camelia *et al.*, *Nature* **393**, 763 (1998).
26. U. Jacob and T. Piran, *JCAP* **01**, 031 (2008).